

# Resistances and Speed Estimation in Sensorless Induction Motor Drives Using a Model with Known Regressors

Jiahao Chen, *Student Member, IEEE*, Jin Huang, and Yan Sun

**Abstract**—This paper addresses the problem of stator and rotor resistances identification in speed sensorless induction motor (IM) drives. The IM model that is transformable into the *adaptive observer form* is sought, for which the speed and rotor resistance adaptive observer can be established with rigorous stability arguments under the assumption of constant unknown parameters. However, further inclusion of stator resistance estimation leads to the over-parametrization problem. As a result, the adaptive observer based on the first-order approximation of the error dynamics is proposed. This is feasible because the regressors of the adopted IM model consist of known signals only. Experiment is carried out to verify the effectiveness of a sensorless drive with the proposed adaptive observer. Compared with the existing methods, speed and resistances estimation during a regeneration mode as well as successful slow speed reversal operation is found possible in the experiments.

**Index Terms**—adaptive observers, induction motors drives, speed sensorless control, stator resistance, rotor resistance, rotor time constant, slow speed reversal.

## I. INTRODUCTION

RECENTLY, a survey on the topic of stator and rotor resistances identification in speed sensorless induction motor (IM) drives is given in [1], where various solutions including adaptive full-order observer [2], model reference adaptive system [3], [4], neural network [5], rotor asymmetry [6], sliding mode [7], [8], extended Kalman filter [9], [10], [11], [12] and those methods based on constructed index [13], [14] are fully reviewed.

The overall conclusion that can be drawn from the literature review is that the online identification of speed, stator resistance and rotor resistance is experimentally realized, but theoretically satisfactory results are absent. Nevertheless, two solutions are found intriguing. The first solution by Marino *et al.* [15] seeks a model representation with which no parameter uncertainty enters the dynamics of unmeasured states, whereas

This work was supported in part by the National Key Basic Research Program of China (973 Project) under Grant 2013CB035604 and in part by the National Natural Science Foundation of China under Grant 51690182.

J. Chen and J. Huang are with the College of Electrical Engineering, Zhejiang University, Hangzhou 310027, China (e-mail: horychen@qq.com). Y. Sun is with the State Grid Nanchang Electric Power Supply Company, Nanchang 330006, China.

the adaptivity to stator resistance is valid only if the mismatch in stator resistance is sufficiently small.

The second solution pursues a model representation that is transformable into the so-called *adaptive observer form*. To this end, an adaptive observer with the electromotive forces as the auxiliary unmeasured states is proposed [1]. However, the proposed dynamics cannot be exactly transformed into the adaptive observer form because the regressors of parameters consist of unknown states (i.e., the electromotive forces). Moreover, the implementation needs the derivative of the stator currents. Although the requirement of current derivative can be dispensed with by choosing another auxiliary states, it in turn causes the problem of over-parametrization.

Apart from the topic of resistances identification, stable low-speed regeneration mode operation of sensorless IM drives is yet another hot topic over the last two decades (see, e.g., [1], [16] for a review). One may expect to use different or time-varying observer coefficients with respect to operating conditions so as to stabilize the sensorless drive. Along this direction, the research usually ends in a set of observer coefficients that rely on the actual motor speed [1], [17], [18], [19], which is unrealistic as stated in [20]. Nevertheless, one promising method that assures the low-speed regenerating operation is the one presented by Montanari *et al.* [21] (see also [22]), of which the stability is guaranteed by a composite observer-controller analysis. However, this method can become sensitive to parameter variations.

As a matter of fact, estimation of resistances during the regeneration region is seldom reported, because the inclusion of resistances identification (especially stator resistance identification) to a speed-adaptive scheme is not a trivial task. In effect, the linearized model based eigenvalue evaluation analysis shows the joint estimation of speed and stator resistance will become unstable for the method proposed in [1]. However, successful estimation of stator resistance [23] or rotor resistance [24] in a regenerating sensorless IM drive is reported but the simultaneous estimation of both stator and rotor resistances is still absent in the literature.

From the authors' point of view, the key to solve the stable sensorless operation and resistances identification in both motoring and regeneration conditions with one set of observer coefficients lies in the introduction of a new IM model (or equivalently a state transformation) to which the existing stability theory can be applied. In this paper, an adaptive design is established based on the new IM model.

TABLE I. List of Symbols

Inverse- $\Gamma$ -circuit Symbols [25]	Notation	Comment
Stator resistance	$r_s$	$3.04 \Omega$
Equivalent rotor resistance	$r_{req}$	$1.60 \Omega$
Equivalent magnetizing inductance	$L_\mu$	$0.448 \text{ H}$
Total leakage inductance	$L_\sigma$	$0.0249 \text{ H}$
Stator inductance	$L_s$	$L_s = L_\mu + L_\sigma$
Stator voltage in $\alpha\beta$ frame	$u_s$	$u_s = [u_{\alpha s}, u_{\beta s}]^T$
Stator current in $\alpha\beta$ frame	$i_s$	$i_s = [i_{\alpha s}, i_{\beta s}]^T$
Equivalent rotor flux (linkage)	$\psi_\mu$	$\psi_\mu = [\psi_{\alpha\mu}, \psi_{\beta\mu}]^T$
Rotor current in $\alpha\beta$ frame	$i_r$	$i_r = L_\mu^{-1} \psi_\mu - i_s$
<hr/>		
New State Variables	Notation	Comment
Total leakage flux	$\psi_\sigma$	$\psi_\sigma = [\psi_{\alpha\sigma}, \psi_{\beta\sigma}]^T$
Equivalent electromotive force	$\chi$	$\chi_\sigma = [\chi_\alpha, \chi_\beta]^T$
<hr/>		
Other Symbols	Notation	Comment
Differentiation operator	$p$	$p = \frac{d}{dt}$
Load torque	$T_L$	-
Reciprocal of the rotor time constant	$\alpha$	$\alpha = r_{req}/L_\mu$
Electrical rotor angular speed	$\omega$	-
Synchronous angular speed	$\omega_\psi$	-
Slip angular speed	$\omega_{sl}$	$\omega_{sl} = \omega_\psi - \omega$
<hr/>		
Derived Symbols	Notation	Comment
Estimated quantities	$\hat{\cdot}$	E.g., $\hat{\psi}_\sigma, \hat{\chi}, \hat{\alpha}, \hat{\omega}, \hat{r}_s$
Error quantities	$\tilde{\cdot}$	E.g., $\tilde{\omega} = \omega - \hat{\omega}$
Computed output error	$\varepsilon$	$\varepsilon = \psi_\sigma - \hat{\psi}_\sigma$

With the proposed adaptive observer, the stable sensorless control during both motoring and regenerating conditions along with online adaptation of both stator and rotor resistances is achieved.

The outline of the paper is as follows. In Sec. II, we introduce the motor dynamics with the set of new state variables, which answers the question raised in [1]. That is, there is a model of IM dynamics that is transformable into the adaptive observer form when speed and rotor resistance are estimated. Nonetheless, the model becomes over-parameterized when it is extended to include stator resistance identification. In Sec. III, thanks to the fact that the regressors of the representation consist of only known signals, the over-parameterized error dynamics are reduced to the linear parameterized ones if we neglect higher order parameter estimated errors. Next, an adaptive observer is devised directly based on the first-order approximation of the error dynamics, which facilitates the stable identification of resistances in both motoring and regenerating sensorless operations. In Sec. IV, effective experiments are carried out, and to distinguish rotor resistance from rotor speed, a time-varying flux modulus command is needed. Finally in Sec V, the conclusion is drawn.

## II. MATHEMATIC MODEL OF IMs

### A. The Conventional Model with Unknown Regressors

The induction motor electrical dynamics in the stationary  $\alpha\beta$  frame are described by the fourth-order equations (1)

$$L_\sigma p i_s = u_s - (r_s + r_{req}) i_s + (\alpha I - \omega J) \psi_\mu \quad (1a)$$

$$p \psi_\mu = r_{req} i_s - (\alpha I - \omega J) \psi_\mu \quad (1b)$$

Please refer to Table I for the definitions of the symbols, and  $I = I_{2 \times 2} = \begin{bmatrix} 1 & 0 \\ 0 & 1 \end{bmatrix}$ ,  $J = \begin{bmatrix} 0 & -1 \\ 1 & 0 \end{bmatrix}$ . Please note that the regressors for rotor resistance and speed contain the unknown states  $\psi_\mu$ .

### B. Parameter Identification Capability

When the IM is under a constant speed and constant flux modulus operation, the motor's electrical state variables (i.e.,  $\psi_\mu$  and  $i_s$ ) are sinusoidal signals, thus from (1) one has

$$L_\sigma p i_s = u_s - r_s i_s - p \psi_\mu \quad (2a)$$

$$p \psi_\mu = \omega_\psi J \psi_\mu \quad (2b)$$

from which one realizes that the motor dynamics (2) are parameterized by stator resistance  $r_s$  and synchronous speed  $\omega_\psi$ , while neither speed  $\omega$  nor rotor resistance  $r_{req}$  appears. As a result, only  $r_s$  and  $\omega_\psi$  are possible to be identified for all model based parameter estimation methods. In fact,  $\omega_\psi$  is a lumped parameter related to  $\omega$  and  $r_{req}$ , because according to the field oriented control one has

$$\omega_\psi - \omega = \omega_{sl} = r_{req} \frac{i_{Ts}}{|\psi_\mu|} = r_{req} \frac{T_L}{n_{pp} |\psi_\mu|^2} \quad (3)$$

where  $i_{Ts}$  is the torque producing current and  $T_L$  the load torque.

On the other hand, comparing (1b) and (2b) yields

$$r_{req} (i_s - L_\mu^{-1} \psi_\mu) = \omega_{sl} J \psi_\mu \quad (4)$$

in which  $L_\mu^{-1} \psi_\mu - i_s = i_r$  is the rotor current. This implies that there is only *rotational electromagnetic force* in the rotor circuits. Furthermore, in the field oriented  $M\text{-}T$  frame<sup>1</sup> it gives

$$(4) \Rightarrow \begin{cases} -r_{req} i_{Mr} = -\omega_{sl} \psi_{T\mu} = 0 \\ -r_{req} i_{Tr} = \omega_{sl} \psi_{M\mu} \end{cases}$$

from which only the ratio between  $r_{req}$  and  $\omega_{sl}$  can be identified. However, one viable option to distinguish  $r_{req}$  from  $\omega$  is to vary the flux modulus so that there will be also *induced electromagnetic force* in the rotor circuits as well. For example, by imposing  $\psi_{M\mu} = m_0 + m_1 \sin(\omega_1 t)$  with  $m_0, m_1, \omega_1$  positive constants, the resulting  $M$ -axis rotor current becomes

$$i_{Mr} = \frac{m_1 \omega_1}{-r_{req}} \cos(\omega_1 t) \neq 0 \quad (5)$$

in which the parameter  $r_{req}$  appears. Hence, the identification of  $r_{req}$  becomes possible.

*Remark:* Here, only an intuitive understanding of the parameter identification capability is made. Curious readers could read [26], [27] for a rigorous analysis with the aid of observability theorem for nonlinear systems.  $\triangle$

### C. The Model with Known Regressors

Introduce the change of state variables as follows [28]

$$\begin{aligned} \psi_\sigma &= L_\sigma i_s \\ \chi &= (\alpha I - \omega J) (L_\sigma i_s + \psi_\mu) \end{aligned} \quad (6)$$

from which the original state variables are recovered by

$$\begin{aligned} i_s &= L_\sigma^{-1} \psi_\sigma \\ \psi_\mu &= (\alpha^2 + \omega^2)^{-1} (\alpha I + \omega J) \chi - \psi_\sigma \end{aligned} \quad (7)$$

<sup>1</sup>In this paper, the  $M\text{-}T$  frame designates the rotor field oriented frame, where  $M$ -axis is aligned with the rotor flux vector while the  $T$ -axis is  $90^\circ$  leading to the  $M$ -axis.

Assuming constant parameters ( $r_s$ ,  $\alpha$  and  $\omega$ ), the electrical dynamics with the new state variables  $\psi_\sigma$  and  $\chi$  follow as

$$\begin{aligned} p\hat{\psi}_\sigma &= \chi - (\alpha L_s + r_s) i_s + \omega J\psi_\sigma + u_s \\ p\chi &= \alpha(u_s - r_s i_s) - \omega J(u_s - r_s i_s) \end{aligned} \quad (8)$$

which is nonlinearly parameterized owing to the coupled parameter terms that involve  $\alpha r_s$  and  $\omega r_s$ .

In the literature, there are adaptive observer design techniques [29], [30], [31] that can be applied for a class of systems whose non-homogeneous part consists of only known signals and is linearly parameterized in unknown parameters. Since the objective is to estimate  $r_s$ ,  $\alpha$  and  $\omega$ , those designs cannot be applied unless we treat the coupled parameter terms  $\alpha r_s$  and  $\omega r_s$  as the fourth and fifth unknown parameters, but this leads to over-parametrization problem.

*Remark:* However, if the objective is to estimate only rotor resistance and speed, those adaptive observer designs can be directly applied because the model (8) is linearly parameterized by  $r_{req}$  and  $\omega$ , and the regressors of  $r_{req}$  and  $\omega$  contain only known signals such as  $r_s$ ,  $L_\sigma$ ,  $L_\mu$ ,  $u_s$  and  $i_s$ .  $\triangle$

### III. ADAPTIVE DESIGN BASED ON ERROR DYNAMICS

In this section, we shift the design focus from the new IM dynamics (8) to the corresponding error dynamics. To this end, we need to first have a candidate observer, and then use a trick to derive the error dynamics that is in first-order approximation linearly parameterized by unknown parameters ( $r_s$ ,  $\alpha$  and  $\omega$ ).

#### A. The Candidate Observer

One candidate full-order observer can be constructed as

$$\begin{aligned} p\hat{\psi}_\sigma &= \hat{\chi} - (\hat{\alpha}L_s + \hat{r}_s)i_s + \hat{\omega}J\psi_\sigma + u_s + k_1\varepsilon \\ p\hat{\chi} &= \hat{\alpha}(u_s - \hat{r}_s i_s) - \hat{\omega}J(u_s - \hat{r}_s i_s) + k_2\varepsilon \end{aligned} \quad (9)$$

where a hat  $\hat{\cdot}$  indicates estimated quantity,  $\varepsilon = \psi_\sigma - \hat{\psi}_\sigma$  is the output error vector, and  $k_1$  and  $k_2$  are positive feedback gains.

#### B. Error Dynamics with the Known Regressors $\Phi$

Subtracting (9) from (8) yields the error dynamics

$$\begin{aligned} p\varepsilon &= -k_1\varepsilon + \tilde{\chi} - i_s \tilde{r}_s - L_s i_s \tilde{\alpha} + J\psi_\sigma \tilde{\omega} \\ p\tilde{\chi} &= -k_2\varepsilon + u_s \tilde{\alpha} - J u_s \tilde{\omega} \\ &\quad - i_s (\alpha r_s - \hat{\alpha} \hat{r}_s) + J i_s (\omega r_s - \hat{\omega} \hat{r}_s) \end{aligned} \quad (10)$$

where we use  $\sim$  to designate the unknown error quantity that represents the difference between actual value and the estimated value, e.g.,  $\tilde{\alpha} = \alpha - \hat{\alpha}$ .

By noticing that

$$\begin{aligned} \hat{\alpha} \hat{r}_s &= \alpha \hat{r}_s - \tilde{\alpha} \hat{r}_s \\ &= \alpha r_s - \alpha \tilde{r}_s - \tilde{\alpha} \hat{r}_s \\ &= \alpha r_s - \hat{\alpha} \tilde{r}_s - \tilde{\alpha} \hat{r}_s - \tilde{\alpha} \hat{r}_s \end{aligned} \quad (11)$$

and similarly that

$$\hat{\omega} \hat{r}_s = \omega r_s - \hat{\omega} \tilde{r}_s - \tilde{\omega} \hat{r}_s - \tilde{\omega} \hat{r}_s, \quad (12)$$

the error dynamics (10) are rewritten in matrix form

$$p \begin{bmatrix} \varepsilon \\ \tilde{\chi} \end{bmatrix} = \begin{bmatrix} -k_1 I & I \\ -k_2 I & 0 \end{bmatrix} \begin{bmatrix} \varepsilon \\ \tilde{\chi} \end{bmatrix} + \Phi \tilde{\theta} + \begin{bmatrix} 0 \\ d(\tilde{\theta}) \end{bmatrix} \quad (13)$$

with the disturbance vector  $d(\tilde{\theta})$ , the parameter error vector  $\tilde{\theta}$ , and the regressor matrix  $\Phi$

$$\begin{aligned} d(\tilde{\theta}) &= -(\tilde{\alpha}I - \tilde{\omega}J)\tilde{r}_s i_s \\ \tilde{\theta} &= [\tilde{r}_s \quad \tilde{\alpha} \quad \tilde{\omega}]^T \\ \Phi &= \begin{bmatrix} -i_s & -L_s i_s & L_\sigma J i_s \\ -\hat{\alpha} i_s + \hat{\omega} J i_s & u_s - \hat{r}_s i_s & -J(u_s - \hat{r}_s i_s) \end{bmatrix} \end{aligned} \quad (14)$$

#### C. The First-order Approximate Error Model

The disturbance vector  $d(\tilde{\theta})$  contains second-order parameter errors of  $\tilde{\alpha}\tilde{r}_s$  and  $\tilde{\omega}\tilde{r}_s$ , which is reasonable to be neglected for limited modelling discrepancy. In fact, similar disposals have been found in literatures (e.g., [32], [15]). As a result, the ensuing adaptive design is based on the first-order approximate error dynamics without the disturbance vector  $d(\tilde{\theta})$ :

$$\begin{aligned} p\tilde{x} &= A\tilde{x} + \Phi\tilde{\theta} \\ \varepsilon &= C\tilde{x} \end{aligned} \quad (15)$$

where  $\tilde{x} = [\varepsilon^T, \tilde{\chi}^T]^T$ ,  $A = \begin{bmatrix} -k_1 I & I \\ -k_2 I & 0 \end{bmatrix}$  and  $C = [I \ 0]$ .

#### D. Parameter Adaptation Rules Design by Intuition

Let  $P$  be a symmetric matrix that makes  $A^T P + PA$  a stable matrix, denote  $\Gamma = \text{diag}(\gamma_{rs}, \gamma_\alpha, \gamma_\omega)$ , and consider a Lyapunov function candidate

$$V = \tilde{x}^T (A^T P + PA) \tilde{x} + \tilde{\theta}^T \Gamma^{-1} \tilde{\theta} \quad (16)$$

whose time derivative follows as

$$\dot{V} = \tilde{x}^T (A^T P + PA) \tilde{x} + 2 \left( \tilde{\theta}^T \Phi^T P \tilde{x} + \tilde{\theta}^T \Gamma^{-1} \dot{\tilde{\theta}} \right) \quad (17)$$

from which, the suggested parameter adaptation rules are apparently

$$\dot{\tilde{\theta}} = -\Gamma \Phi^T P \tilde{x} \quad (18)$$

which are, however, infeasible because of the dependence on  $\tilde{\chi}$  (recall that  $\tilde{x} = [\varepsilon^T, \tilde{\chi}^T]^T$ ). It is of interest to see whether the system is still stable after replacing (18) with the simplified rules as

$$\dot{\tilde{\theta}} = -\Gamma \Phi^T \varepsilon \quad (19)$$

Then,  $\dot{V}$  becomes

$$\dot{V} \stackrel{(19)}{=} \tilde{x}^T (A^T P + PA) \tilde{x} + 2\tilde{\theta}^T \Phi^T (P\tilde{x} - \varepsilon) \quad (20)$$

which implies  $\tilde{x}$  is input-to-state stable provided that the disturbance  $\tilde{\theta}$  is bounded (see, e.g., [33, Theorem 4.19]). Furthermore,  $\tilde{x}$  is asymptotically stable in the limit when  $\tilde{\theta}$  vanishes. Now, the question is whether the simplified adaptive rules (19) is asymptotically stable.

### E. The Stable Parameter Adaptation Rules

Regarding  $\Phi\tilde{\theta}$  as the inputs, the transfer functions to  $\varepsilon$  are derived from (15)

$$\begin{aligned}\varepsilon &= G(p)\Phi\tilde{\theta} \equiv C(pI_{4 \times 4} - A)^{-1}\Phi\tilde{\theta} \\ &= \frac{1}{p^2 + k_1p + k_2} \begin{bmatrix} pI & I \end{bmatrix} \Phi\tilde{\theta}\end{aligned}\quad (21)$$

with  $G(p) \triangleq C(pI - A)^{-1}$ . Substituting (21) into (19) yields

$$\dot{\tilde{\theta}} = -\Gamma\Phi^T \left\{ \frac{1}{p^2 + k_1p + k_2} \begin{bmatrix} pI & I \end{bmatrix} \Phi\tilde{\theta} \right\} \quad (22)$$

According to [34, Theorem 2.3], we cannot conclude the asymptotical stability of  $\tilde{\theta}$  from (22), since neither  $\frac{1}{p^2 + k_1p + k_2}$  nor  $\frac{p}{p^2 + k_1p + k_2}$  is a strictly positive real function.

As a matter of fact, in order to derive the asymptotically stable parameter adaptation rules, we are bound to filter the original regressor  $\Phi$  so that the lemma of [29, Lemma 1] will apply. To this end, we introduce the effective output error  $\varepsilon_{\text{eff}}$

$$\begin{aligned}\varepsilon_{\text{eff}} &\triangleq \varepsilon + G(p)\Phi\hat{\theta} - [G(p)\Phi]\hat{\theta} \\ &= G(p)\Phi\theta - [G(p)\Phi]\hat{\theta} \\ &= [G(p)\Phi]\tilde{\theta}\end{aligned}\quad (23)$$

in which we emphasize that signals  $[G(p)\Phi] \in \mathbb{R}^{2 \times 3}$  are generated by applying  $G(p)$  to  $\Phi$ , while signals  $G(p)\Phi\hat{\theta} \in \mathbb{R}^2$  are produced by applying  $G(p)$  to  $\Phi\hat{\theta}$ , that is,  $[G(p)\Phi]\hat{\theta} \neq G(p)\Phi\hat{\theta}$ .

The stable parameter adaptation rules are consequently devised by

$$\begin{aligned}p\hat{\theta} &= \Gamma[G(p)\Phi]^T\varepsilon_{\text{eff}} \\ &= \Gamma[G(p)\Phi]^T[G(p)\Phi]\tilde{\theta}\end{aligned}\quad (24)$$

with  $\hat{\theta} = [\hat{r}_s \ \hat{\alpha} \ \hat{\omega}]^T$ , which is asymptotically stable if the filtered regressor  $[G(p)\Phi]$  is persistently exciting, i.e., the matrix  $[G(p)\Phi]^T[G(p)\Phi]$  is in integral sense a bounded positive definite matrix, i.e., there exist positive constants  $a, b, T$  such that, for all  $t$ , the following inequalities hold:

$$bI_{3 \times 3} \geq \int_t^{t+T} [G(p)\Phi]^T(t)[G(p)\Phi](t)dt \geq aI_{3 \times 3}, \quad (25)$$

Finally, as the norm of  $\tilde{\theta}$  decreases, it is not difficult to show from (20) (with Barbalat's lemma) that the trajectory of  $\tilde{x}$  will also converge towards 0 in the limit of null  $\tilde{\theta}$ .

### F. Brief Summary

So far, the adaptive observer design is complete. The 4<sup>th</sup>-order observer is given in (9), and the 3<sup>rd</sup>-order stable adaptation rules are designed in (24). The calculation of the effective output error  $\varepsilon_{\text{eff}}$  needs extra auxiliary states, i.e., the  $\mathbb{R}^2$  vector  $G(p)\Phi\hat{\theta}$  and the  $\mathbb{R}^{2 \times 3}$  matrix  $[G(p)\Phi]$ . How they are generated will be explicitly shown as follows. Let

$$\eta \triangleq G(p)\Phi\hat{\theta} \quad (26)$$

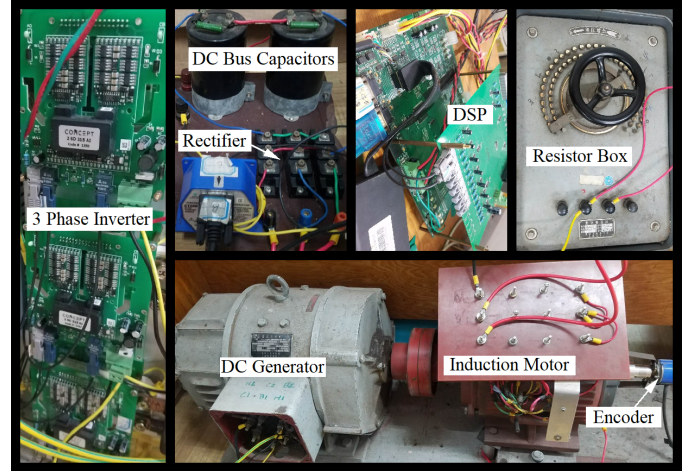


Fig. 2. Photos of the experimental system.

Then signal  $\eta$  is computed by

$$\begin{aligned}p \begin{bmatrix} \eta \\ \varsigma \end{bmatrix} &= \begin{bmatrix} -k_1I & I \\ -k_2I & 0 \end{bmatrix} \begin{bmatrix} \eta \\ \varsigma \end{bmatrix} \\ &+ \begin{bmatrix} -i_s\hat{r}_s - L_s i_s \hat{\alpha} + L_\sigma J_i_s \hat{\omega} \\ (-\hat{\alpha}i_s + \hat{\omega}J_i_s)\hat{r}_s + (u_s - \hat{r}_s i_s)\hat{\alpha} - J(u_s - \hat{r}_s i_s)\hat{\omega} \end{bmatrix}\end{aligned}\quad (27)$$

with  $\varsigma \in \mathbb{R}^2$  as an auxiliary state. Let

$$\begin{aligned}\Upsilon &= [v^1 \ v^2 \ v^3] \triangleq G(p)\Phi \\ &= \frac{1}{p^2 + k_1p + k_2} \begin{bmatrix} (-pi_s - \hat{\alpha}i_s + \hat{\omega}J_i_s)^T \\ (-L_s p i_s + u_s - \hat{r}_s i_s)^T \\ (J p \psi_\sigma - Ju_s + J\hat{r}_s i_s)^T \end{bmatrix}^T\end{aligned}\quad (28)$$

with  $v^1, v^2, v^3 \in \mathbb{R}^2$ . Then matrix  $\Upsilon$  can be determined in components as follows

$$\begin{aligned}p \begin{bmatrix} v^1 \\ \zeta^1 \\ v^2 \\ \zeta^2 \\ v^3 \\ \zeta^3 \end{bmatrix} &= \begin{bmatrix} -k_1I & I \\ -k_2I & 0 \\ -k_1I & I \\ -k_2I & 0 \\ -k_1I & I \\ -k_2I & 0 \end{bmatrix} \begin{bmatrix} v^1 \\ \zeta^1 \\ v^2 \\ \zeta^2 \\ v^3 \\ \zeta^3 \end{bmatrix} + \begin{bmatrix} -i_s \\ -\hat{\alpha}i_s + \hat{\omega}J_i_s \\ -L_s i_s \\ u_s - \hat{r}_s i_s \\ -JL_\sigma i_s \\ -J(u_s - \hat{r}_s i_s) \end{bmatrix}\end{aligned}\quad (29)$$

with  $\zeta^1, \zeta^2, \zeta^3 \in \mathbb{R}^2$  as auxiliary states.

There are 5 design coefficients (i.e.,  $k_1, k_2, \gamma_{rs}, \gamma_\alpha, \gamma_\omega$ ). The adaptive observer is dependent on  $L_\mu, L_\sigma$ , and the initial values of  $r_s, \alpha$  and  $\omega$ ; its inputs are  $u_s$  and  $i_s$ ; its outputs are  $\hat{\psi}_\sigma, \hat{\chi}, \hat{r}_s, \hat{\alpha}$  and  $\hat{\omega}$ . The estimation of rotor resistance is obtained by computing  $\hat{r}_{req} = L_\mu\hat{\alpha}$ . A block diagram of the adaptive observer is sketched in Fig. 1a.

## IV. EXPERIMENT RESULTS

### A. Experimental System Setup

The proposed scheme is implemented in the digital signal processor TMS320F28335. The sampling frequency is 4 kHz. The induction motor, whose nameplate data are 4 kW, 1440 rpm, 380 V and 8.8 A, is driven by a voltage-source inverter. The load torque is provided by a separately excited dc generator, and it is computed by  $T_L = K_{dcl}i_{Load}$  with

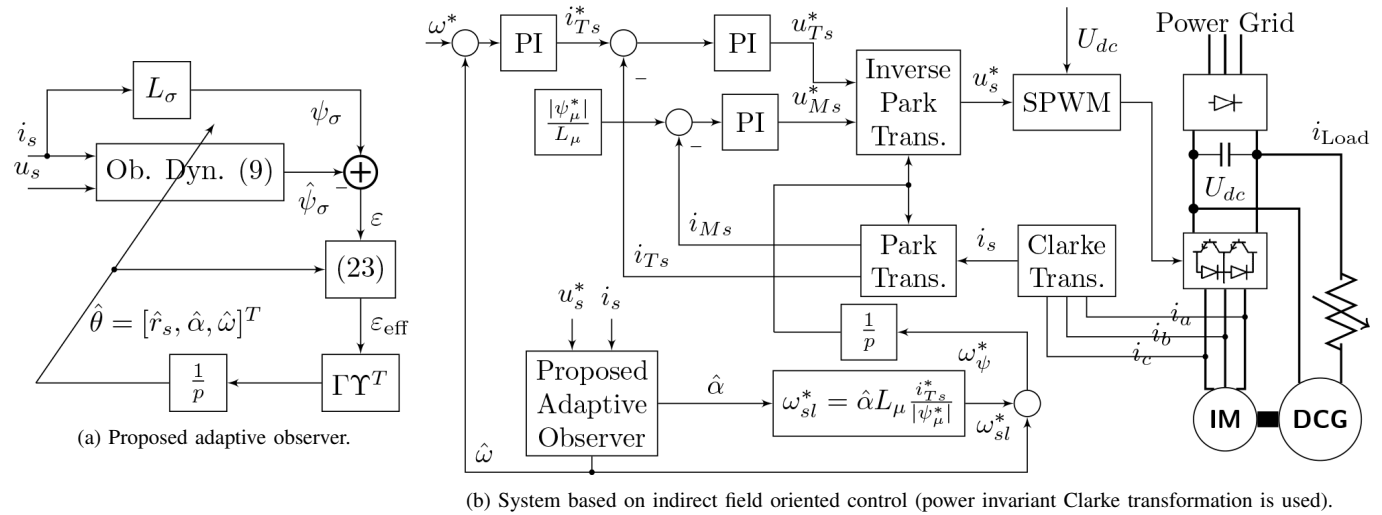


Fig. 1. Block diagrams of the whole sensorless control system.

$K_{dc}$  the dc torque factor and  $i_{Load}$  the measured armature current. Particularly, the regenerative load torque is produced by connecting the armature of the dc generator to the dc bus. The numerical values of the tested motor is listed in Table I, while the observer coefficients are given in Appendix. The control structure is sketched in Fig. 1b, and the pictures of the test stand is shown in Fig. 2.

### B. Practical Consideration for Avoiding Resistances Identification in Speed Transients

Large oscillations in resistances estimation can be observed if  $\hat{r}_s$  and  $\hat{r}_{req}$  are updated during speed transients. It is because that for adaptive observer based joint speed and resistances estimation, the indicator of mismatched resistances is the output error  $\varepsilon = \psi_\sigma - \hat{\psi}_\sigma$ , which is also the indicator of biased speed estimation and the unmodeled dynamics:

- (1) Biased speed estimation. Variation of speed, which breaks the assumption  $p\omega = 0$ , is equivalent to constantly setting new initial error of speed estimation, such that the output error  $\varepsilon$  is constantly disturbed by the speed estimated error.
- (2) The unmodeled dynamics. The proposed observer is based on the model assuming constant parameters (i.e.,  $p\omega = pr_{req} = pr_s = 0$ ). During the speed transient where  $p\omega \neq 0$ , the unmodeled dynamics appear in  $p\chi$ :

$$p\chi = (\alpha I - \omega J)(u_s - r_s i_s) - \dot{\omega} J \psi_s$$

That is to say, even if we set  $\hat{\omega} = \omega$ , the output error  $\varepsilon$  is still disturbed.

As a result, if resistances identification is activated during speed transient, no accurate estimation results can be assured. Hence, updating of estimation of resistances during speed transient is discouraged for the proposed method.

*Remark:* However, a few papers have reported positive results [12], [35], [36], [37]. Specifically, In [36], the relation between rotor resistance and slip frequency is acquired in off-line tests. In [37], estimated  $q$ -axis flux is used to tune rotor resistance but the speed measurement is required. In [12],

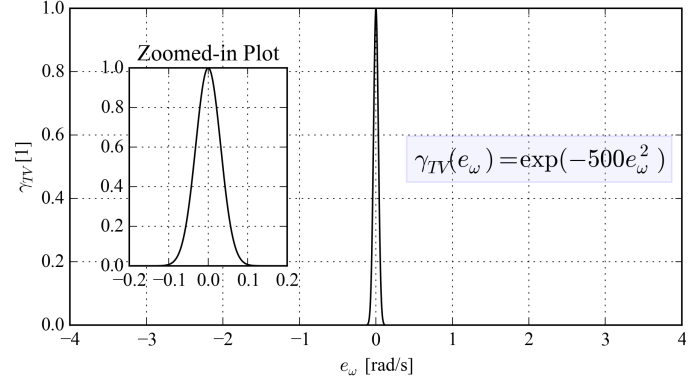


Fig. 3. Function  $\gamma_{TV}(e_\omega)$ .

presented is the sensorless experimental results of resistances estimation during speed transient using the switching EKF algorithm. In [35], a particular indicator of rotor resistance error is put forth. △

In order to automatically turn off the resistance identification during speed transient, we introduce the time-varying gain matrix  $\Gamma'$  in replace of the constant gain matrix  $\Gamma$ :

$$\Gamma'(t) = \text{diag}(\gamma_{TV}\gamma_{rs}, \gamma_{TV}\gamma_\alpha, \gamma_\omega) \quad (30)$$

where we select the time-varying gain as

$$\gamma_{TV} = \exp(-500e_\omega^2) \quad (31)$$

with  $e_\omega = \omega^* - \hat{\omega}$  the speed control error. A plot of the function  $\gamma_{TV}(e_\omega)$  is given in Fig. 3.

### C. Verification of Resistances Identification

According to the discussion of the last sub-section, the objective is then to estimate both stator and rotor resistances at steady state so as to improve the speed control accuracy of the sensorless drive. Thus, in order to show the effectiveness of the proposed adaptive observer, the experiment under variation in both  $r_s$  and  $r_{req}$  is carried out, and the results are shown in Fig. 4.

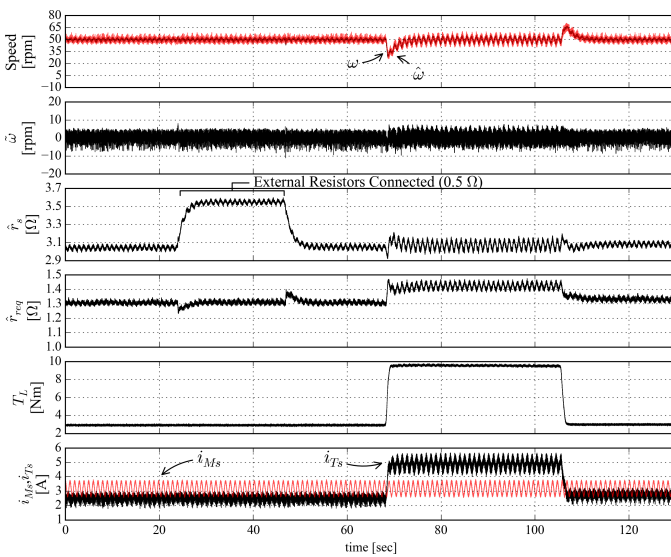


Fig. 4. Experimental verification of stator and rotor resistances identification: Drive behaviors with respect to external resistors and sudden load change. (Estimated speed is used for speed control.)

In the experiment, to verify the effectiveness of the stator resistance estimation, we connect (at  $t = 24$  sec) and remove (at  $t = 46$  sec) the external three phase resistors of  $0.5 \Omega$  between the stator terminals and inverter output. As seen from Fig. 4, the waveform of  $\hat{r}_s$  tracks the step variation of the actual  $r_s$ , and  $\hat{r}_{req}$  is disturbed by the step variation of  $r_s$ .

As for rotor resistance estimation, since the rotor resistance is known to be a function of slip frequency for squirrel-cage IMs, we apply a sudden load change to vary the slip frequency of the motor. As shown in Fig. 4 when  $t \in [68, 107]$  sec, the value of  $\hat{r}_{req}$  increases as the load torque gets heavier.

The low frequency oscillations in  $\hat{\omega}$ ,  $\hat{r}_s$ ,  $\hat{r}_{req}$  and  $i_{Ts}$  are caused by the low frequency (1 Hz) sinusoidal component in the magnetizing current command  $i_{Ms}^*$ . According to Sec. II-B, such excitation is crucial for improving the parameter identification capability of the sensorless drive, i.e., it is crucial for distinguishing rotor resistance from rotor speed.

#### D. Sensorless Slow Speed Reversal Test

Sensorless slow speed reversal is an effective way to exhibit the stability of speed estimation during motoring and regenerating operations [16], [38], and it is carried out for the proposed system (see Fig. 5). As is stated before, resistances identification is suspended during the speed reversal, and their values are set to their nominal values during this test. From the test results shown in Fig. 5, one observes that the speed estimation deviates near the vicinity of zero stator frequency (i.e.,  $\omega_\psi \approx 0$ ). As a consequence, incorrect speed estimation causes biased orientation of the rotor field, so the change in torque producing current  $i_{Ts}$  does not contribute to the expected proportional increase in motor torque. However, successful sensorless slow speed reversal is still realized.

#### E. Sensorless High Speed Operation

In Fig. 6, presented are the experimental results of the proposed sensorless drive in flux weakening region. The torque

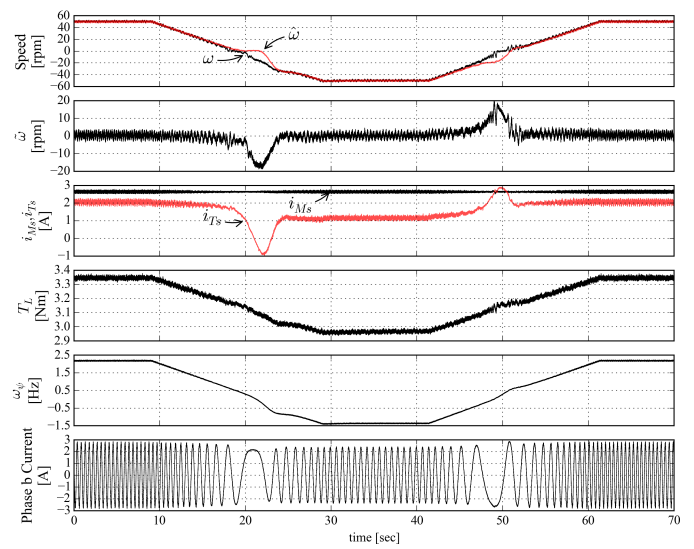


Fig. 5. Sensorless slow speed reversal test.

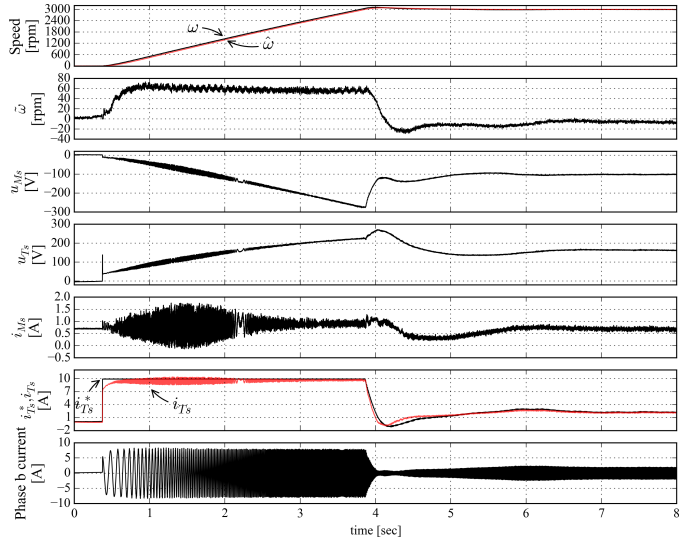


Fig. 6. Sensorless high speed operation: Step response to the speed command of 3000 rpm.

current limit is 10 A. It takes around 3.5 sec to reach the step speed command of 3000 rpm. Speed estimated error is about 60 rpm during the speed transient, while it reduces towards 0 rpm after the speed command is reached. The results verify the effectiveness of the speed estimation.

#### F. Sensorless Control with Resistances Identification

In Fig. 7, the sensorless control experiments are conducted to verify the stability of the simultaneous estimation of  $\omega$ ,  $r_s$ ,  $r_{req}$  in both motoring and regenerating conditions. Furthermore, deliberate step detuning of both  $\hat{r}_s$  and  $\hat{r}_{req}$  is imposed at  $t = 14$  sec in order to test the system robustness with respect to uncertainty of resistances. When the load is light, detuned resistances have limited impact on speed estimation performance, whereas apparent oscillation and bias in speed estimation are observed after the load torque of  $T_L \approx 10$  Nm is applied at  $t = 22$  sec. At  $t = 29$  sec, the adaptation of resistances is activated. As a result, the actual speed converges

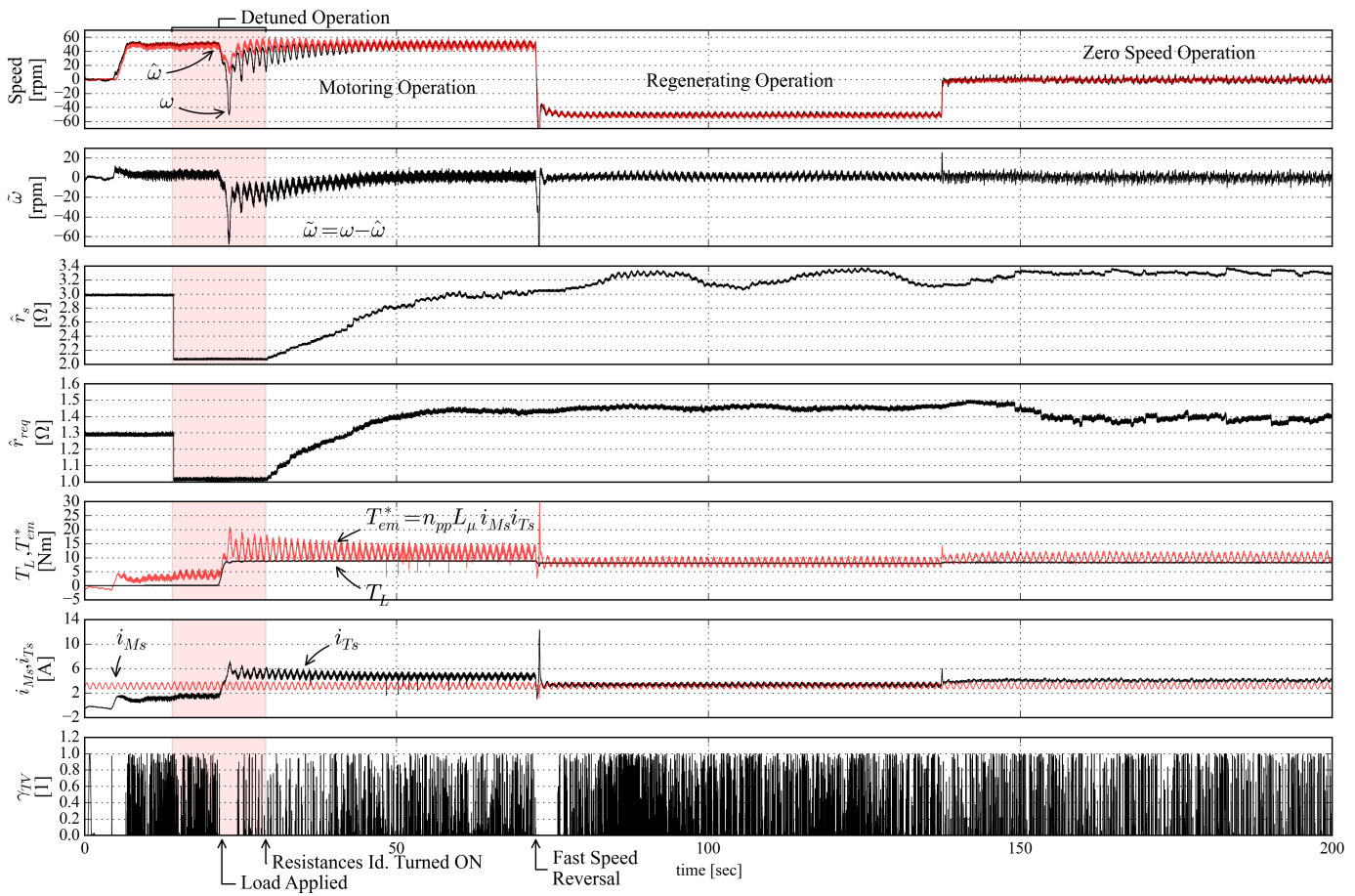


Fig. 7. Sensorless control experiments with stator and rotor resistances identification at motoring, regenerating and zero-speed operations.

towards the estimated speed as the estimation of resistances is updated. In addition, owing to the existence of friction, calculated torque  $T_{em}^*$  is not equal to the load torque computed by the armature current of the dc generator.

At  $t = 72$  sec, a fast speed reversal is performed, and it shows that the proposed speed estimation can track fast speed variation. After the speed reversal, the motor operates stably in regenerating operation, and the adaptation of resistances improves the speed estimation accuracy. Finally at  $t = 137$  sec, the motor begins to operate stably at zero speed, and again, speed estimation accuracy is improved by online updating of resistances.

Thanks to the introduction of  $\gamma_{TV}$ , estimation of resistances is not disturbed by speed transient and load torque change. As seen from Fig. 7, resistances identification is automatically suspended when the motor starts, when the load is applied, and when the fast speed reversal is executed.

Overall, we conclude that with the proposed adaptive observer, the sensorless IM drive can achieve fast/slow speed reversal as well as wide speed range operation, and the steady state accuracy of speed estimation and control is improved by online updating of both stator and rotor resistances. However, during the transient, the estimation of resistances must be suspended via the using of time-varying gain  $\gamma_{TV}$ , or else the drive performance will be deteriorated with adaptation of resistances.

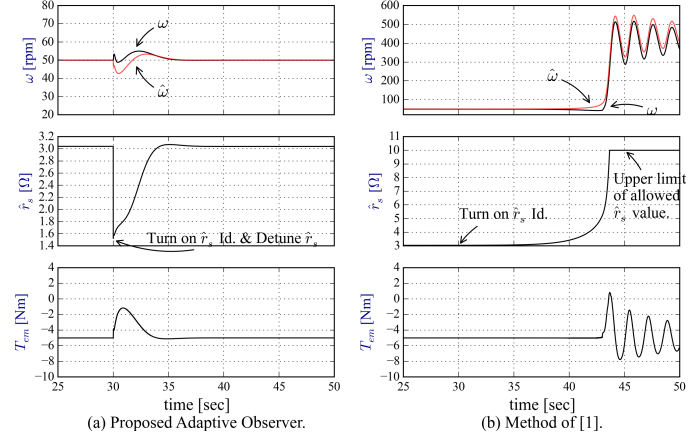


Fig. 8. Comparison simulations for joint speed and stator resistance estimation in regeneration mode. (Sensorless control is implemented.)

## V. CONCLUSION AND DISCUSSION

This paper uses an IM model that has known regressors. In virtue of the model, a speed adaptive observer is proposed, which also provides accurate estimation of stator and rotor resistances during both motoring and regenerating operations. In the meanwhile, the resulting speed sensorless drive survives during a slow speed reversal test. Although deviation of speed estimation does occur when the stator frequency is near the vicinity of zero, the fast crossing of zero frequency

is found to be stable. According to the experiment results, we conclude that with the proposed adaptive observer, the admissible operation range is widened and the robustness of the sensorless drive is as well improved.

Compared to the past work [1], the proposed adaptive observer has the following advantages:

- (1) No differentiation of stator currents is needed.
- (2) No extra analysis on speed estimation in regeneration mode is needed.
- (3) Resistances identification along with speed estimation in regeneration mode is realized.

In Fig. 8, results of a simulated comparison study between the proposed adaptive observer and the method of [1] are presented. It is observed that the introduction of stator resistance identification in regeneration mode, deteriorates the performance of the sensorless drive in [1] [Fig. 8(b)]. As a comparison, the proposed sensorless drive stays stable in regeneration mode even under a step detuning of stator resistance [Fig. 8(a)].

## APPENDIX

### EXPERIMENT SPECIFICATION

The observer coefficients are (in SI units):  $k_1 = 1000$ ,  $k_2 = 16000$ ,  $\gamma_{rs} = 5e6$ ,  $\gamma_\alpha = 5e6$ ,  $\gamma_\omega = 5e7$ . The coefficients are determined in numerical simulation studies by trial and error method. However, a simple procedure can be followed:

- (1) The feedback gains  $k_1$  and  $k_2$  should first be decided, to reach a fast convergence rate of states estimation.
- (2) Then, the speed estimation is tuned to be able to track the actual speed, when the actual speed is used in control.
- (3) Finally, the gains for adaptation of resistances are determined. Generally, a slow adaptation is suggested to make the system stay robust [34].

## REFERENCES

- [1] J. Chen and J. Huang, "Stable simultaneous stator and rotor resistances identification for speed sensorless induction motor drives: Review and new results," *IEEE Transactions on Power Electronics*, vol. PP, no. 99, pp. 1–1, 2017.
- [2] H. Tajima, G. Guidi, and H. Umida, "Consideration about problems and solutions of speed estimation method and parameter tuning for speed-sensorless vector control of induction motor drives," *Industry Applications, IEEE Transactions on*, vol. 38, no. 5, pp. 1282–1289, 2002.
- [3] J. Chen and J. Huang, "Online decoupled stator and rotor resistances adaptation for speed sensorless induction motor drives by a time-division approach," *IEEE Transactions on Power Electronics*, vol. 32, no. 6, pp. 4587–4599, June 2017.
- [4] J. Chen, J. Huang, and M. Ye, "Totally adaptive observer for speed sensorless induction motor drives: Simply a cost of extra energy consumption," in *2017 IEEE International Electric Machines and Drives Conference (IEMDC)*, May 2017, pp. 1–7.
- [5] B. Karanayil, M. F. Rahman, and C. Grantham, "Online stator and rotor resistance estimation scheme using artificial neural networks for vector controlled speed sensorless induction motor drive," *IEEE Transactions on Industrial Electronics*, vol. 54, no. 1, pp. 167–176, Feb 2007.
- [6] L. Zhao, J. Huang, J. Chen, and M. Ye, "A parallel speed and rotor time constant identification scheme for indirect field oriented induction motor drives," *IEEE Transactions on Power Electronics*, vol. 31, no. 9, pp. 6494–6503, Sept 2016.
- [7] L. Zhao, J. Huang, H. Liu, B. Li, and W. Kong, "Second-order sliding-mode observer with online parameter identification for sensorless induction motor drives," *Industrial Electronics, IEEE Transactions on*, vol. 61, no. 10, pp. 5280–5289, 2014.
- [8] G. Tarchaa and T. Orowska-Kowalska, "Equivalent-signal-based sliding mode speed mras-type estimator for induction motor drive stable in the regenerating mode," *IEEE Transactions on Industrial Electronics*, vol. 65, no. 9, pp. 6936–6947, Sept 2018.
- [9] M. Barut, S. Bogosyan, and M. Gokasan, "Switching ekf technique for rotor and stator resistance estimation in speed sensorless control of ims," *Energy Conversion and Management*, vol. 48, no. 12, pp. 3120 – 3134, 2007. [Online]. Available: <http://www.sciencedirect.com/science/article/pii/S0196890407001252>
- [10] ———, "Experimental evaluation of braided ekf for sensorless control of induction motors," *IEEE Transactions on Industrial Electronics*, vol. 55, no. 2, pp. 620–632, Feb 2008.
- [11] M. Barut, "Bi input-extended kalman filter based estimation technique for speed-sensorless control of induction motors," *Energy Conversion and Management*, vol. 51, no. 10, pp. 2032 – 2040, 2010. [Online]. Available: <http://www.sciencedirect.com/science/article/pii/S0196890410001032>
- [12] M. Barut, R. Demir, E. Zerdali, and R. Inan, "Real-time implementation of bi input-extended kalman filter-based estimator for speed-sensorless control of induction motors," *IEEE Transactions on Industrial Electronics*, vol. 59, no. 11, pp. 4197–4206, Nov 2012.
- [13] L. Zhen and L. Xu, "Sensorless field orientation control of induction machines based on a mutual mras scheme," *IEEE Transactions on Industrial Electronics*, vol. 45, no. 5, pp. 824–831, 1998.
- [14] I.-J. Ha and S.-H. Lee, "An online identification method for both stator- and rotor resistances of induction motors without rotational transducers," *IEEE Transactions on Industrial Electronics*, vol. 47, no. 4, pp. 842–853, Aug 2000.
- [15] R. Marino, T. Patrizio, and M. C. Verrelli, *AC Electric Motors Control: Advanced Design Techniques and Applications*. Wiley Online Library, 2013, ch. Adaptive Output Feedback Control of Induction Motors, pp. 158–187.
- [16] L. Harnefors and M. Hinkkanen, "Stabilization methods for sensorless induction motor drives — a survey," *IEEE Journal of Emerging and Selected Topics in Power Electronics*, vol. 2, no. 2, pp. 132–142, June 2014.
- [17] S. Suwankawin and S. Sangwongwanich, "A speed-sensorless im drive with decoupling control and stability analysis of speed estimation," *IEEE Transactions on Industrial Electronics*, vol. 49, no. 2, pp. 444–455, Apr 2002.
- [18] ———, "Design strategy of an adaptive full-order observer for speed-sensorless induction-motor drives-tracking performance and stabilization," *IEEE Transactions on Industrial Electronics*, vol. 53, no. 1, pp. 96–119, Feb 2006.
- [19] M. S. Zaky, M. k. Metwally, H. Azazi, and S. Deraz, "A new adaptive smo for speed estimation of sensorless induction motor drives at zero and very low frequencies," *IEEE Transactions on Industrial Electronics*, vol. PP, no. 99, pp. 1–1, 2018.
- [20] E. Etien, C. Chaigne, and N. Bensiali, "On the stability of full adaptive observer for induction motor in regenerating mode," *IEEE Transactions on Industrial Electronics*, vol. 57, no. 5, pp. 1599–1608, May 2010.
- [21] M. Montanari, S. M. Peresada, C. Rossi, and A. Tilli, "Speed sensorless control of induction motors based on a reduced-order adaptive observer," *IEEE Transactions on Control Systems Technology*, vol. 15, no. 6, pp. 1049–1064, Nov 2007.
- [22] M. Montanari, S. Peresada, and A. Tilli, "A speed-sensorless indirect field-oriented control for induction motors based on high gain speed estimation," *Automatica*, vol. 42, no. 10, pp. 1637 – 1650, 2006. [Online]. Available: <http://www.sciencedirect.com/science/article/pii/S0005109806002172>
- [23] M. Saejia and S. Sangwongwanich, "Averaging analysis approach for stability analysis of speed-sensorless induction motor drives with stator resistance estimation," *IEEE Transactions on Industrial Electronics*, vol. 53, no. 1, pp. 162–177, Feb 2006.
- [24] M. Montanari, A. Tilli, and C. Rossi, "Sensorless indirect field oriented control of induction motors with rotor resistance adaptation," in *2007 European Control Conference (ECC)*, July 2007, pp. 5753–5760.
- [25] G. R. Slemon, "Modelling of induction machines for electric drives," *IEEE Transactions on Industry Applications*, vol. 25, no. 6, pp. 1126–1131, Nov 1989.
- [26] R. Marino, P. Tomei, and C. M. Verrelli, *Induction motor control design*. Springer Science & Business Media, 2010.
- [27] P. Vaclavek, P. Blaha, and I. Herman, "Ac drive observability analysis," *Industrial Electronics, IEEE Transactions on*, vol. 60, no. 8, pp. 3047–3059, 2013.

- [28] Y. Zheng and K. A. Loparo, "Adaptive flux and speed estimation for induction motors," in *Proceedings of the 1999 American Control Conference (Cat. No. 99CH36251)*, vol. 4, 1999, pp. 2521–2525 vol.4.
- [29] Q. Zhang, "Adaptive observer for multiple-input-multiple-output (mimo) linear time-varying systems," *IEEE Transactions on Automatic Control*, vol. 47, no. 3, pp. 525–529, Mar 2002.
- [30] P. Kudva and K. S. Narendra, "Synthesis of an adaptive observer using lyapunov's direct method," *International Journal of Control*, vol. 18, no. 6, pp. 1201–1210, 1973. [Online]. Available: <http://dx.doi.org/10.1080/00207177308932593>
- [31] R. Marino and P. Tomei, "Global adaptive observers for nonlinear systems via filtered transformations," *IEEE Transactions on Automatic Control*, vol. 37, no. 8, pp. 1239–1245, Aug 1992.
- [32] F. Jadot, F. Malrait, J. Moreno-Valenzuela, and R. Sepulchre, "Adaptive regulation of vector-controlled induction motors," *Control Systems Technology, IEEE Transactions on*, vol. 17, no. 3, pp. 646–657, 2009.
- [33] H. K. Khalil, *Nonlinear systems*, 3rd. Prentice Hall, 2002, vol. 9.
- [34] B. D. Anderson, R. R. Bitmead, C. R. J. Johnson, P. V. Kokotovic, R. L. Kosut, I. M. Mareels, L. Praly, and B. D. Riedle, *Stability of Adaptive Systems: Passivity and Averaging Analysis*. Cambridge, MA: MIT Press, 1986.
- [35] K. Akatsu and A. Kawamura, "Online rotor resistance estimation using the transient state under the speed sensorless control of induction motor," *IEEE Transactions on Power Electronics*, vol. 15, no. 3, pp. 553–560, May 2000.
- [36] A. B. Proca and A. Keyhani, "Identification of variable frequency induction motor models from operating data," *IEEE Transactions on Energy Conversion*, vol. 17, no. 1, pp. 24–31, Mar 2002.
- [37] C. Mastorocostas, I. Kioskeridis, and N. Margaris, "Thermal and slip effects on rotor time constant in vector controlled induction motor drives," *IEEE Transactions on Power Electronics*, vol. 21, no. 2, pp. 495–504, March 2006.
- [38] J. Chen and J. Huang, "Globally stable speed-adaptive observer with auxiliary states for sensorless induction motor drives," *IEEE Transactions on Power Electronics*, pp. 1–1, 2018.



**Jiahao Chen** (S'17) was born in Wenzhou, China, in 1991. He received the B.Sc. degree in electrical engineering from Zhejiang University, Hangzhou, China, in 2014, where he is currently working toward the Ph.D. degree in electrical engineering with the College of Electrical Engineering.

His research interests include estimation and control of electric motors and bearingless motors.



**Jin Huang** received the B.Sc. degree in electrical engineering from Zhejiang University, Hangzhou, China, in 1982, and the Ph.D. degree in electrical engineering from the National Polytechnic Institute of Toulouse, Toulouse, France, in 1987. From 1987 to 1994, he was an Associate Professor with the College of Electrical Engineering, Zhejiang University. Since 1994, he has been a Professor at Zhejiang University.

His research interests include electrical machine, ac drives, multiphase machine, and motor parameter identification.



**Yan Sun** was born in Nanchang, China, in 1965. She received the B.Sc. degree in electrical engineering from Jiangxi University of Technology, Nanchang, China, in 1986. She is now a senior engineer in State Grid Nanchang Electric Power Supply Company.

Her research interests include design and operation of electrical appliances.